TYPE Original Research
PUBLISHED 18 May 2023
DOI 10.3389/fmats.2023.1181356



OPEN ACCESS

EDITED BY
Eugenio Pedullà,
University of Catania, Italy

REVIEWED BY
Taha Özyürek,
Bahçeşehir University, Türkiye
António Ginjeira,
University of Lisbon, Portugal

*CORRESPONDENCE
Van-Khoa Pham,
✉ khoapv@ump.edu.vn

RECEIVED 07 March 2023
ACCEPTED 09 May 2023
PUBLISHED 18 May 2023

CITATION
Pham V-K (2023), Dynamic cyclic fatigue resistance of NiTi instruments in a double-curved stainless steel canal with variable distances of displacement.
*Front. Mater.* 10:1181356.
doi: 10.3389/fmats.2023.1181356



# Dynamic cyclic fatigue resistance of NiTi instruments in a double-curved stainless steel canal with variable distances of displacement

Van-Khoa Pham*

Department of Operative Dentistry and Endodontics, Faculty of Odonto-Stomatology, University of Medicine and Pharmacy at Ho Chi Minh City, Ho Chi Minh City, Vietnam

The present study aimed to measure the number of cycles to fracture (NCF) of different instruments using pecking motion at constant and varying distances of movement at body temperature. This study included 20 files from each brand: ProTaper Universal F2, ProTaper Next X2, and WaveOne Gold Primary (Dentsply Sirona, Maillefer, Ballaigues, Switzerland). Instruments from each brand were divided into two groups (ten files for each group) that experienced constant or variable distances in a stainless-steel artificial double-curved canal in a platform that ensured that the instrument rotated at a stable temperature with a minimum fluctuation of the environment. While running, the platform was programmatically controlled to move at any desired distance of instrument displacement to simulate the clinical pecking motion at variable distances. The files were rotated using proprietary programs. The times to fracture were recorded and then transformed into the number of cycles to fracture (NCF). Data were analyzed using Minitab with proper tests. All fragments were observed under a scanning electron microscope to capture and describe the characteristics of the fracture surface. The WaveOne Gold had the highest NCF, while the ProTaper Universal had the lowest NCF. The manufacturer brands and the modes of displacement of the experimental instrument showed interactive effects. The fracture surface revealed no striation. A new design, material, mode of rotation, and different distances of movement have certain effects on the cyclic fatigue resistance of the instrument.

KEYWORDS

**nickel–titanium (NiTi), cyclic fatigue, pecking motion, body temperature, reciprocating, ProTaper Universal, ProTaper Next, WaveOne Gold**

## Background

Endodontic nickel–titanium (NiTi) rotary instruments provide useful characteristics for resolving complicated situations in contemporary root canal therapy (Thu et al., 2020). The most troublesome accident for this flexible instrument is breakage during endodontic preparation (La Rosa et al., 2021a). Many factors with mechanisms involving complex combinations affect instrument fracture in canal enlargement (Liang and Yue, 2022). With the advancement of technologies in cross-sectional design, production, surface treatment, thermal process, metallurgy, and motion mode, many rotary endodontic NiTi instruments have been developed with improved resistance to cyclic fatigue (Liang and Yue, 2022). The manipulation of endodontic instruments with dynamic motion is recommended to minimize the ratio of instrument failure in the clinical setting (Liang and Yue, 2022).

To simulate the clinical setting, previous studies have developed and tested many improvements (Topçuoğlu et al., 2020; Zubizarreta-Macho et al., 2020; La Rosa et al., 2021b; Faus-Matoses et al., 2022). The resistance of cyclic fatigue by endodontic instruments is evaluated in static or dynamic situations (Thu et al., 2020) with both in-and-out or pecking motions (Galeti et al., 2020; Thu et al., 2020; Zubizarreta-Macho et al., 2020). While the static situation has certain advantages and supplies invaluable outcomes, it does not reflect the exact clinical situation and seems to shorten the cyclic fatigue time of the instruments (Hülsmann et al., 2019). Therefore, the dynamic platform is more suitable than the static condition for fatigue testing (Hülsmann et al., 2019).

Room temperature, which ranges from 20°C to 25°C, is not related to the clinical setting, although several studies were performed under this condition (Topçuoğlu et al., 2020; La Rosa et al., 2021a). These data should be provided by the manufacturer, and the body temperature environment seems more appropriate in cyclic fatigue research (Hülsmann et al., 2019).

The ProTaper Universal (PTU), ProTaper Next (PTN), and WaveOne Gold (WOG) (Dentsply Sirona, Maillefer, Ballaigues, Switzerland) are well-established and popular endodontic instruments that have been available for many years. The material of the PTU is conventional NiTi, whereas the material of the PTN is an M-wire that experiences pre-production heat treatment of NiTi. The WOG is manufactured of NiTi Gold, a post-production heat-treated NiTi. Both of the former devices offer continuous rotation, while the latter offers movement of reciprocation, a new mode of rotation in the desire for reducing the fracture rate. Many previous studies, in many situations, demonstrated the cyclic fatigue and torsional resistance of these instruments.

While a previous study assessed the cyclic fatigue resistance of endodontic instruments with different distances of pecking motion (Galeti et al., 2020), this kind of motion is not similar to that in the clinical setting. The constant-distance pecking motion is also improper.

The present study aimed to measure the number of cycles to the breakage of different instruments using a pecking motion at a constant distance and different amplitudes of movement.

The null hypothesis was that there was no difference among the NCFs of the three experimental groups for different modes of displacement.

## Methods

The sample size was calculated using the result of the previous pilot study with an alpha value of 0.05 and a power of 0.99. The effect size in the pilot study was 2.3, resulting in a sample size of 9 for every group. In the present study, 10 instruments were chosen for each experimental group. Twenty files for each brand of the PTU, PTN, and WOG were selected for the present study. The files were checked under a dental operating microscope at 10× magnification (CJ Optik GmbH and Co. KG, Aßlar-Werdorf, Germany) for any damage or imperfections on the material's surface. A platform containing gear for the endodontic motor holder and a glass box of sewing machine oil was created to test the instruments (Figure 1). A digital controller was designed and fabricated to set the movements of a stainless-steel block containing the double-curved canal following any modes. The mode of motion was set as in-and-out with a step-in of 1 mm from the second curved position until the tip of the instrument reached the apex and then repeated to instrument fracture. The glass box contained oil (Shell Morlina 10, Shell Corp., Ho Chi Minh City, Viet Nam) to maintain temperature and lubricate the instrument when rotated inside the stainless-steel canal. The temperature of the glass box was kept stable by using a heating device combined with a digital temperature controller and a thermal sensor to control the on/off of the heating device.

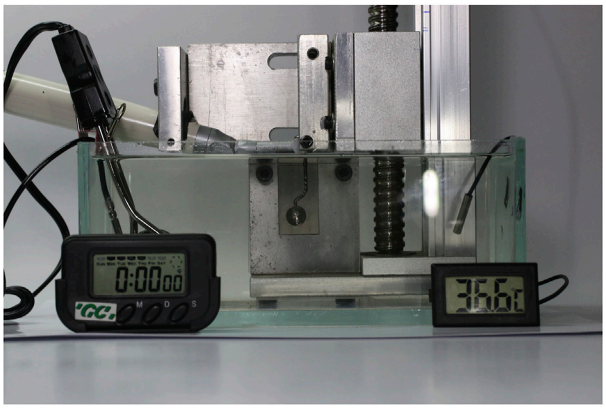

FIGURE 1
Platform of the experimental setup.

The stainless-steel block containing the artificial canal was produced using a special technique for S-curved or double-curved canals. The stainless-steel block was immobilized in the glass box of sewing machine oil. The handpiece of the endodontic motor was fixed on the gear designed especially for the X-Smart Plus (Dentsply Sirona, Maillefer, Ballaigues, Switzerland). The gear was driven by a step motor with a digital controller that can be programmed as desired by the researcher. The gear can be displaced in or out at any distance for each kind of motion, as programmed by the operator and controlled through an LCD interface with function keys.

A stopwatch was set in front of the glass box, and an iPhone was used to record the entire process from the beginning of rotation until the breakage of the file. The time was recorded for the rotation of the intact file and multiplied by the round per minute of each kind of instrument, as instructed by the manufacturer, for the number of cycles. All fragments were observed under a scanning electron microscope to capture and describe the characteristic of the fracture surface.

## Results

The statistical data on the number of cycles to fracture of each instrument system are displayed in Table 1.

**TABLE 1 Descriptive statistics of the NCF for each experimental instrument.**

| Descriptive statistics | PTU 1 | PTU 2 | PTN 1 | PTN 2 | WOG 1 | WOG 2 |
|---|---|---|---|---|---|---|
| Goodness-of-fit Anderson–Darling (adjusted) | 1.484 | 1.688 | 1.496 | 1.730 | 1.744 | 1.456 |
| Distribution | Lognormal | Normal | Weibull | Lognormal | Lognormal | Lognormal |
| Mean | 499.658[a] | 669.577[b] | 884.078[c] | 1413.65[d] | 1760.87[e] | 2428.65[f] |
| Standard deviation | 173.022 | 54.3672 | 186.341 | 434.314 | 333.302 | 567.437 |
| Median | 472.152 | 669.577 | 895.847 | 1351.31 | 1730.15 | 2364.96 |

1: Dynamic cycles with constant displacement distances. 2: Dynamic cycles with variable displacement distances. [a, b, c, d, e, f] Different superscript letters for significant differences among the groups ($p < 0.05$). The NCF of the ProTaper Universal was the lowest of the six experimental groups.

**TABLE 2 Numbers of fragments for each experimental group.**

| Number of fragments | PTU 1 | PTU 2 | PTN 1 | PTN 2 | WOG 1 | WOG 2 |
|---|---|---|---|---|---|---|
| 1 | 10 | 4 | 8 | 10 | 10 | 10 |
| 2 | 0 | 6 | 2 | 0 | 0 | 0 |
| *p* | a | b* | ab | a | a | a |

1: Dynamic cycles with constant displacement distances. 2: Dynamic cycles with variable displacement distances. [a, ab] $p > 0.05$, [b*, ab] $p > 0.05$, [a, b*] $p < 0.05$ Fisher's exact tests.

**TABLE 3 Regression of live data: NCF versus dynamic cycle brands and types.**

| Predictor | Coefficient | Standard error | Z | *p* | 95.0% normal CI | |
|---|---|---|---|---|---|---|
| | | | | | Lower | Upper |
| Intercept | 6.146835 | 0.0615542 | 99.86 | <0.0001* | 6.026191 | 6.267479 |
| Brand | | | | | | |
| PTN | 0.657474 | 0.0753882 | 08.72 | <0.0001* | 0.509716 | 0.805232 |
| WOG | 1.281958 | 0.0753882 | 17.00 | <0.0001* | 1.134200 | 1.429716 |
| Types of dynamic cycles | | | | | | |
| Variable distances | 0.366891 | 0.0615542 | 05.96 | <0.0001* | 0.246247 | 0.487535 |
| Scale | 0.238398 | 0.0217627 | | | 0.199342 | 0.285107 |

*$p < 0.05$: significant difference. The regression of live data showed differences among the experimental groups. The brands and types of dynamic cycles were the factors affecting the NCF in the groups in the present study.

**TABLE 4 Phases in which the breakage happened for each instrument system.**

| Phase | PTU 1 | PTU 2 | PTN 1 | PTN 2 | WOG 1 | WOG 2 |
|---|---|---|---|---|---|---|
| In | 2 | 9 | 1 | 6 | 1 | 5 |
| Out | 0 | 1 | 2 | 2 | 1 | 2 |
| At the full length | 8 | 6 | 9 | 2 | 8 | 3 |
| *p*/Cramer's V | 0.011*/0.026 | | | | | |

1: Dynamic cycles with constant displacement distances. 2: Dynamic cycles with variable displacement distances. *$p < 0.05$, Fisher's exact test. The experimental groups showed significant differences in the phases during which the fracture occurred.

The number of fragments for each experimental instrument system is displayed in Table 2.

The regression with live data on the NCF versus brands and types of dynamic cycles is displayed in Table 3.

The phases in which the fracture occurred for each experimental group are displayed in Table 4.

The SEM images of the fracture surfaces of each brand in dynamic cycles with constant displacement distances are

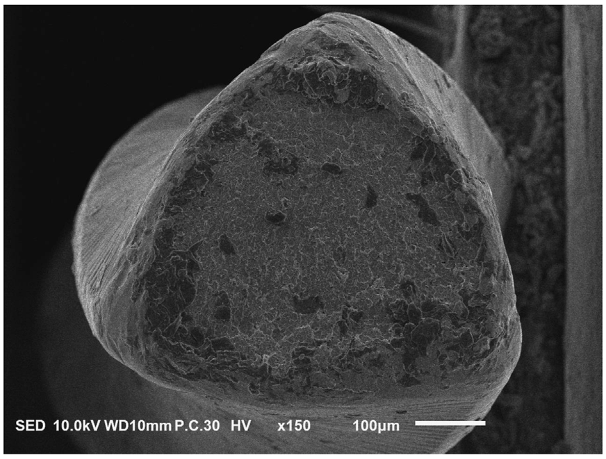


FIGURE 2
PTU F1 fracture surface at 150× magnification.

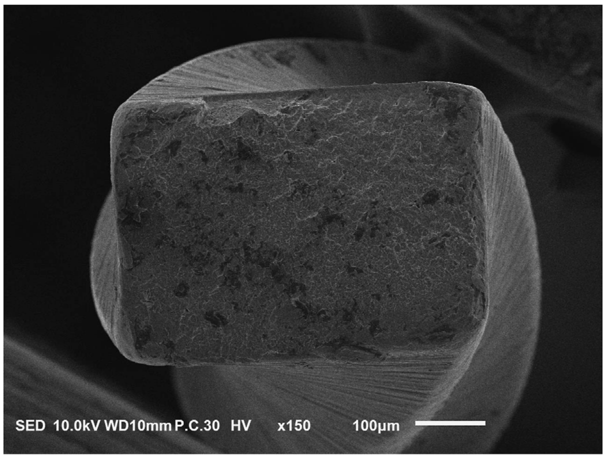


FIGURE 4
PTN X2 fracture surface at 150× magnification.

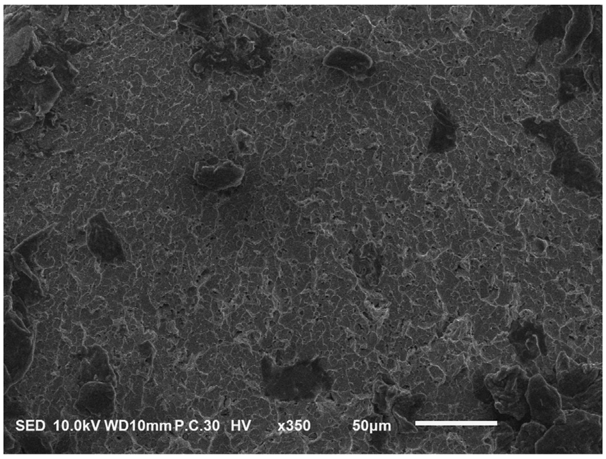


FIGURE 3
PTU F1 fracture surface at 350× magnification.

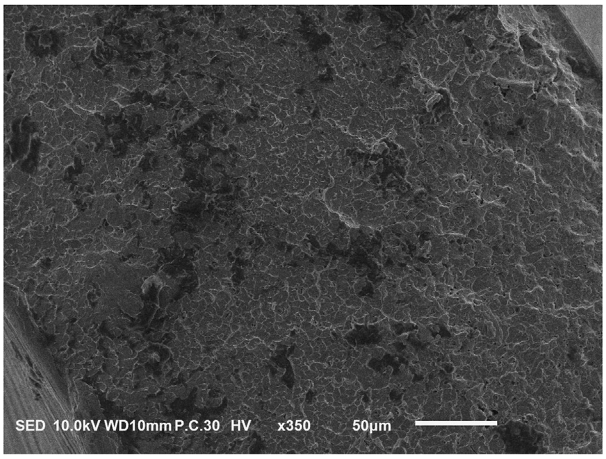


FIGURE 5
PTN X2 fracture surface at 350× magnification.

displayed in Figures 2–7. There is no striation on all the images of the fracture surface.

## Discussion

The results of the present study showed that the reciprocating rotary instrument in dynamic cycles with variable displacement distances yielded the highest NCF in the body temperature environment. The simulated pecking motion with the fixed increase of 1 mm per motion in the present condition was nearly similar to the clinical setting, which no other previous study mentioned. The in–out motion with constant distance at the full length of the artificial canal did not produce significantly better NCF for the NiTi instrument compared with the pecking motion with variable displacement distances. The distributions of data for each experimental instrument system appeared to be normal; however, these distributions were not suitable for the reliability analysis in Minitab software, as displayed in Table 1.

Unlike previous studies, not all the instruments in the present study were broken into two fragments in the double-curved artificial canal. The eight instruments were broken into two fragments with a total of 60 experimental instruments. The *p*-value of the Fisher exact test was <0.05; therefore, there was a correlation between the manufacturer brand and the modes of displacement with the number of fragments, as shown in Table 2.

The results of the regression with life data in the reliability analysis in Minitab (Table 3) revealed that the brands of the manufacturer and the modes of displacement of the experimental instrument had interactive effects because all *p* were <0.05. The

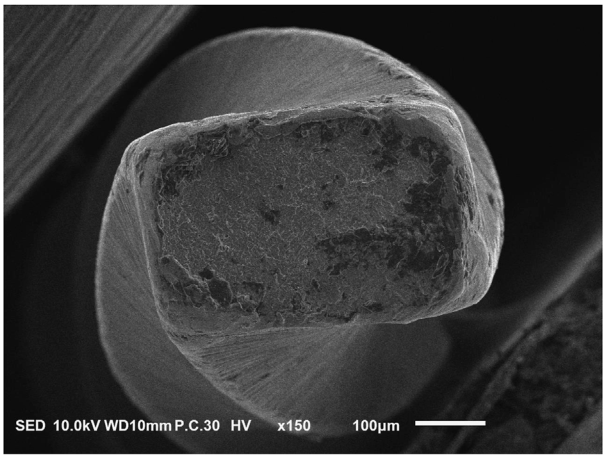


FIGURE 6
WOG primary fracture surface at 150× magnification.

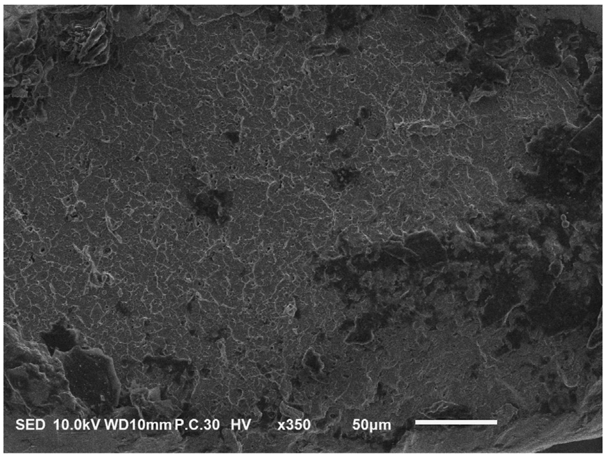


FIGURE 7
WOG primary fracture surface at 350× magnification.

*p*-value for the PTN was <0.05, and the coefficient (0.657474) was positive; therefore, the NCF of the PTN was higher than that of the PTU. The *p*-value for the WOG was <0.05, and the coefficient (1.281958) was positive; therefore, the NCF of the WOG was higher than that of the PTU. The coefficient for the WOG was higher than that for the PTN, and the NCF of the WOG was higher than that of the PTN. The *p*-value for the variable distances mode was <0.05, and the coefficient (0.366891) was positive; therefore, the NCF of the instrument used in this mode of displacement was higher than that of the instrument in the constant distance mode.

The phase in which the file is broken when used inside the canal is an important factor in cyclic fatigue investigation. However, previous studies did not mention this phenomenon in their results or discussions. The results of the present study revealed that almost all instruments broke at the full length of the artificial canal. However, the instruments could break during both in- or out-phase when rotated in the canal, regardless of the mode of displacement (constant or variable distances). The *p*-value of the Fisher exact test was <0.05, as displayed in Table 4. A correlation was observed between the brands and the modes of displacement of the experimental instrument.

One of the most important issues whenever stainless-steel canals are used is the hardness of the material used for the production of the canal. If the material is not properly treated during the thermal process, the hardness is not high enough to keep the right outline of the canal, leading to the improper movement of the instrument during the testing procedure. The time to fracture of the instrument will be expanded whenever there is a fault in the stainless-steel canal wall because of the in-and-out motion of the file inside the canal, resulting in improper outcomes for the tested instrument.

Another issue is the temperature of the environment in which the instrument rotates, including the motor. Bbody temperature was chosen for simulating the most appropriate clinical setting. Although the augmentation of the entire room temperature is an easier and more convenient way to perform experiments, high environmental temperatures create an uncomfortable feeling for the researcher and have an adverse effect on the normal operation of the sensitive endodontic motor. The sewing machine oil used in the present study is the most appropriate environment to maintain a stable temperature and lubricate instrument movement inside the stainless-steel canal. This oil is colorless, odorless, and tasteless and is appropriate for clear vision and motion capture. Oil also helps maintain a stable temperature in an isolated glass box containing the experimental artificial canal and instrument and minimize the fluctuation of the temperature during testing time. The use of a glass box containing the clear oil did not permit the integration of an LED into the canal wall to automatically detect instrument fracture during the testing period. However, file breakage was easily observed by following the tracing of the video playback. The time to fracture of the file can be cross- and double-checked based on the times displayed on the screen of the video recorder and the digital clock.

A heating oil device is easily equipped alongside a temperature controller, resulting in a stable temperature system in the present experiment.

The reciprocating mode of the endodontic motor is apparently not designed for long working sessions. The motor will stop suddenly with no warning signs. This may be a protective function from the manufacturer. In the pilot study, the motor stopped in certain situations. However, with the proper room temperature, somewhere between 20°C and 23°C, the motor did not stop during the testing period, assuring reliable results.

The order of the fractures on the tip of the instrument was normal, although in the pilot study, in some circumstances, breakage of the second curved position occurred first. While this phenomenon is extremely rare, it did happen. Under other circumstances, such as the different distances between the two curved positions or from the apex to the first curved position, there will be abnormal breakage of the instrument. Fortunately, for most situations in the clinical setting, the longer the breakage section, the easier the removal procedure.

SEM microphotography of the fracture surface revealed no striation on the image, consistent with findings reported previously (Jamleh et al., 2019). Fatigue fracture without striation might occur under certain circumstances (Committee, and Fractography, A. H., 1987; González-Velázquez, 2018; Faus-

Matoses et al., 2022). Creep fatigue interactions could contribute to the mechanism of the formation of fractography of breakage on the surface without striation under the circumstance in the present study (González-Velázquez, 2018). This result differs from that of the previous study (Jamleh et al., 2019).

The limitations of the present study include the lack of evaluation of the cyclic fatigue resistance of different endodontic instruments in different modes of in-and-out movement. Moreover, the platform was designed only for body temperature.

Further investigations should be performed to assess the cyclic fatigue of other rotary nickel–titanium files in many other modes of in-and-out movement with different amplitudes of motion. Other curved angles and positions should be tested on the same platform to cover more situations simulating the clinical setting.

## Data availability statement

The original contributions presented in the study are included in the article/Supplementary Material. Further inquiries can be directed to the corresponding author.

## Author contributions

V-KP designed and performed the study. The author confirms being the sole contributor of this work and has approved it for publication.

## Conflict of interest

The author declares that the research was conducted in the absence of any commercial or financial relationships that could be construed as a potential conflict of interest.

## Publisher's note

All claims expressed in this article are solely those of the authors and do not necessarily represent those of their affiliated organizations, or those of the publisher, the editors, and the reviewers. Any product that may be evaluated in this article, or claim that may be made by its manufacturer, is not guaranteed or endorsed by the publisher.

## References


Committee, and Fractography, A. H. (1987). *ASM international*.

Faus-Matoses, V., Faus-Llácer, V., Ruiz-Sánchez, C., Jaramillo-Vásconez, S., Faus-Matoses, I., and Martín-Biedma, B. (2022). Effect of rotational speed on the resistance of NiTi alloy endodontic rotary files to cyclic fatigue—an *in vitro* study. *J. Clin. Med.* 11, 3143. doi:10.3390/jcm11113143

Galeti, G. G., Soares, A. J., Mendes, E. B., and Frozoni, M. R. (2020). Influence of different distances of pecking motion on cyclic fatigue resistance of reciproc blue files. *Int. J. Adv. Eng. Res. Sci.* 7, 162–167. doi:10.22161/ijaers.711.19

González-Velázquez, J. L. (2018). "Fatigue fracture," in *Fractography and failure analysis* (Cham: Springer International Publishing). 71-95.

Hülsmann, M., Donnermeyer, D., and Schäfer, E. (2019). A critical appraisal of studies on cyclic fatigue resistance of engine-driven endodontic instruments. *Int. Endod. J.* 52, 1427–1445. doi:10.1111/iej.13182

Jamleh, A., Alghaihab, A., Alfadley, A., Alfawaz, H., Alqedairi, A., and Alfouzan, K. (2019). Cyclic fatigue and torsional failure of EdgeTaper platinum endodontic files at simulated body temperature. *J. Endod.* 45, 611–614. doi:10.1016/j.joen.2019.02.008

La Rosa, G. R. M., Palermo, C., Ferlito, S., Isola, G., Indelicato, F., and Pedullà, E. (2021). Influence of surrounding temperature and angle of file access on cyclic fatigue resistance of two single file nickel-titanium instruments. *Aust. Endod. J.* 47, 260–264. doi:10.1111/aej.12473

La Rosa, G. R. M., Shumakova, V., Isola, G., Indelicato, F., Bugea, C., and Pedullà, E. (2021). Evaluation of the cyclic fatigue of two single files at body and room temperature with different radii of curvature. *Materials* 14, 2256. doi:10.3390/ma14092256

Liang, Y., and Yue, L. (2022). Evolution and development: Engine-driven endodontic rotary nickel-titanium instruments. *Int. J. Oral Sci.* 14, 12. doi:10.1038/s41368-021-00154-0

Thu, M., Ebihara, A., Maki, K., Miki, N., and Okiji, T. (2020). Cyclic fatigue resistance of rotary and reciprocating nickel-titanium instruments subjected to static and dynamic tests. *J. Endod.* 46, 1752–1757. doi:10.1016/j.joen.2020.08.006

Topçuoğlu, H. S., Topçuoğlu, G., Kafdağ, Ö., and Balkaya, H. (2020). Effect of two different temperatures on resistance to cyclic fatigue of one Curve, EdgeFile, HyFlex CM and ProTaper next files. *Aust. Endod. J.* 46, 68–72. doi:10.1111/aej.12369

Zubizarreta-Macho, Á., Mena Álvarez, J., Albaladejo Martínez, A., Segura-Egea, J. J., Caviedes Brucheli, J., Agustín-Panadero, R., et al. (2020). Influence of the pecking motion frequency on the cyclic fatigue resistance of endodontic rotary files. *J. Clin. Med.* 9, 45. doi:10.3390/jcm9010045